J. Fluid Mech. (2008), *vol.* 607, *pp.* 279–288. © 2008 Cambridge University Press
doi:10.1017/S0022112008002218 Printed in the United Kingdom

Passive locomotion of a simple articulated fish-like system in the wake of an obstacle

JEFF D. ELDREDGE AND DAVID PISANI

Mechanical & Aerospace Engineering Department, University of California, Los Angeles, Los Angeles, CA 90095-1597, USA

(Received 28 March 2008 and in revised form 12 May 2008)

The behaviour of a passive system of two-dimensional linked rigid bodies in the wake of a circular cylinder at $Re = 100$ is studied computationally. The three rigid bodies are connected by two frictionless hinges, and the system ('fish') is initially aligned with a streamwise axis three diameters behind the cylinder. Once flow symmetry is broken, the wake rolls up into a Kármán vortex street in which the fish is stably trapped, and the passing large-scale vortices induce an undulatory shape change in the articulated system. It is found that, for certain fish lengths relative to cylinder diameter, the fish is propelled upstream toward the cylinder. Furthermore, the fish is propelled equally effectively when the hinges are locked, confirming that induced body undulation is not necessary for achieving a net thrust. An analysis of the forces on constituent bodies shows that leading-edge suction and negative skin friction on the forward portion of the fish are in competition with positive skin friction on the aft portion; propulsion is achieved when the forebody contributions dominate those on the aftbody. It is shown that the so-called 'suction zone' behind the cylinder that enables this passive propulsion is double the length of that without a fish present.

1. Introduction

Many aquatic creatures employ techniques that rely on the ambient flow environment to reduce their own energy expenditure. For example, it is generally accepted that river fish hold station in particular locations of streams, such as in wakes and in low-speed regions adjacent to shear layers, partly to take advantage of the flow behaviour (Fausch & White 1981; Fausch 1993; Webb 1998). Many of the field observations were clarified in laboratory experiments (Liao *et al.* 2003) with a live rainbow trout in a water flume with a vertically oriented cylinder. Not only did the fish seek refuge behind the cylinder, but it also tended to synchronize its body motion with – and possibly extract energy from – the coherent vortices shed from the cylinder. Such beneficial use of adjacent vortices may also be used by fish in schools (Weihs 1973).

Observations such as those by Liao *et al.* (2003), beyond their intrinsic scientific value, offer intriguing possibilities for the design of efficient autonomous underwater vehicles, particularly those that are designed to operate in groups. Such applications motivate a more detailed study of extraction of energy from vortical flows and the beneficial use of this energy for propulsion. The actual degree to which energy is extracted from the wake is difficult to measure in a live fish, but the energetic motion of a dead fish in the wake is undeniably passive. Beal *et al.* (2006) performed carefully controlled experiments on a dead trout in the wake of an obstacle to demonstrate that energy can be extracted from large-scale coherent vortices in order to 'swim' upstream.

After a short interval, the dead fish was observed to travel toward the cylinder, during which the fish's undulations were synchronized with the vortex passage frequency.

The passively extracted energy from the wake may also be converted into electricity, such as in the energy-harvesting 'eel' studied by Allen & Smits (2001). This investigation explored the deformation of a tethered piezoelectric membrane in the near-wake of a bluff body. The proximity of the long membrane to the base of the cylinder inhibited large-scale vortex formation in Reynolds numbers below 10^3, and deformation was correspondingly negligible. However, the vortical wake induced large-amplitude undulations in the membrane at Reynolds numbers larger than $\sim 10^4$. Furthermore, the amplitude of lateral oscillation was larger than the width of the membraneless wake, suggesting that the membrane's deformation tended to enlarge the wake vortices.

The shape change imparted by the vortical wake to the flexible structure is remarkably similar to the undulatory swimming mode in elongated organisms. However, swimming in a train of vortices is not the same as swimming in a quiescent medium, and it is not obvious that these basic mechanics will generate thrust in the wake. To complicate matters, there is more than one potential propelling mechanism. Beal *et al.* (2006) distinguished between the thrust generated by 'slaloming' between wake vortices and the thrust developed when the leading edge breaches the region of cylinder base suction. Because the objective of their study was to isolate the slaloming thrust mechanism in the dead fish, special attention was devoted to ensuring that the fish was initially placed downstream of the so-called 'suction zone' of the cylinder. This zone was defined in their study as the complement of the region in which the velocity field was uniformly and perpetually tilted downstream. They determined from particle image velocimetry data of the wake (apparently without the fish) that the suction zone's boundary lay approximately 1.75 diameters downstream of the obstacle base, and consequently they placed the fish four diameters downstream.

The present computational study of passive locomotion in the wake is conducted with the goal of examining the mechanisms of locomotion in greater detail than is possible in experiments. This study is not intended to reproduce the experiments of Beal *et al.* (2006) – the simulations reported in this paper are two-dimensional, the 'fish' is an articulated system of linked rigid bodies, and the Reynolds number is substantially smaller. Rather, the problem, which is described in § 2, is treated abstractly as a streamlined deformable system in the wake of an obstacle. The results of several studies that explore the effects of fish length and rigidity, the forces exerted on the fish, and the flow environment in which the fish resides, are reported in § 3.

2. Problem set-up

The problem's initial configuration is depicted in figure 1. A cylinder of diameter D is immersed in a uniform free stream of velocity U. An articulated 'fish' of overall length L and with density equal to that of the fluid is placed at a distance d downstream of the cylinder and at a height $h = 0.25D$ above the centreline in order to break the symmetry of the problem. In all cases presented here, the fish consists of three identical ellipses, each of aspect ratio five, joined by two passive hinges which are transparent to the flow. The ellipse nearest the cylinder is labelled the 'forebody' and the farthest ellipse is the 'aftbody'. Penetrable gaps of width $0.2D$ are allowed between adjacent ellipses in order to mitigate the singular behaviour of the numerical method as two surface panels become too close. These gaps do, in fact, have some effect on the resulting flow, though the basic behaviour is not significantly affected by their presence.

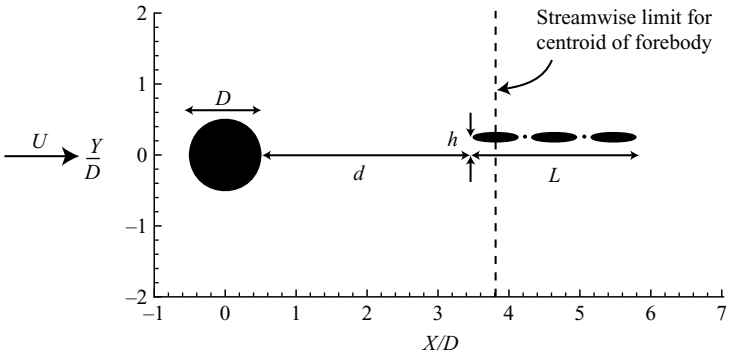

FIGURE 1. Initial configuration of cylinder and three-link fish.

For all cases considered in this paper, the streamwise separation distance, d, is fixed at $3D$. This value was chosen as a compromise between formulating a computationally practical problem and placing the fish downstream of the expected suction region directly behind the cylinder. (As will be shown in § 3.4, the latter is not actually achieved.) In order to prevent the fish from being swept downstream by the initial incident flow, a streamwise limit was imposed on the centroid of the forebody of the fish at its initial placement; the fish was unrestricted both in transverse motion and in rotation. In the previous experiments by Beal *et al.* (2006), the dead fish was attached to the cylinder by a string that became taut at a length of $4D$.

The Reynolds number for the simulations, based on cylinder diameter and free-stream velocity, is 100. The incompressible Navier–Stokes equations were solved with a viscous vortex particle method with coupled fluid–body dynamics (Eldredge 2008). The numerical parameters were chosen to ensure that results were converged. Note that, because of its particle-based nature, the numerical method does not require a truncated computational domain. This approach ensures that the flow is not affected by artificial boundaries; however, it also limits the duration of the simulations, since the number of computational elements increases as the vortical wake grows. The simulations reported here were long enough to analyse the mechanisms of passive propulsion.

3. Results and discussion

An example of the basic behaviour of the fish is shown in figure 2, which depict the vorticity field and the instantaneous configuration of the system for a fish of length $L = 2.275$. The hinges of this fish are free to rotate without frictional or elastic resistance. After the vortical wake of the cylinder reaches and surrounds it, the fish moves downward toward the centreline. At approximately $tU/D = 13.76$, the fish begins to move toward the cylinder; at the same time, the symmetry of the wake is broken, and alternating Kármán vortex shedding is initiated. By $tU/D = 26.4$, the left-most point ('head') of the fish has travelled approximately 1.1 cylinder diameters upstream. The fish is stably trapped between the vortices for the entire duration of the simulation. The shape of the fish is clearly influenced by the passing vortical flow, as is evident in the evolving angles of the individual constituent bodies plotted in figure 3. The rotation of the centrebody and aftbody always lag that of the forebody, and, after the onset of alternating vortex shedding, the rotational amplitude grows with each successive body.

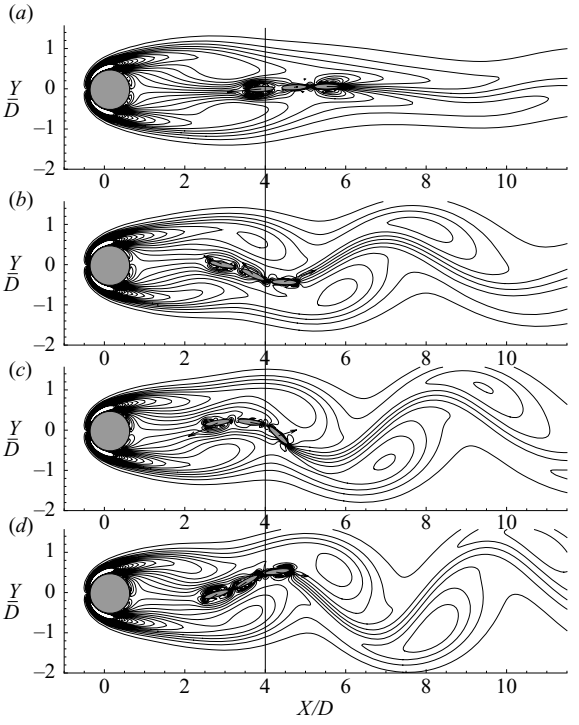

FIGURE 2. Snapshots of the configuration and vorticity field for a free-hinge fish of length $L = 2.275D$ at four different instants: (*a*) $tU/D = 13.76$, (*b*) 24.64, (*c*) 26.40, (*d*) 28.08. The vertical line corresponds to the original streamwise position of the centroid of the forebody. Instantaneous force vectors on each constituent body are also shown.

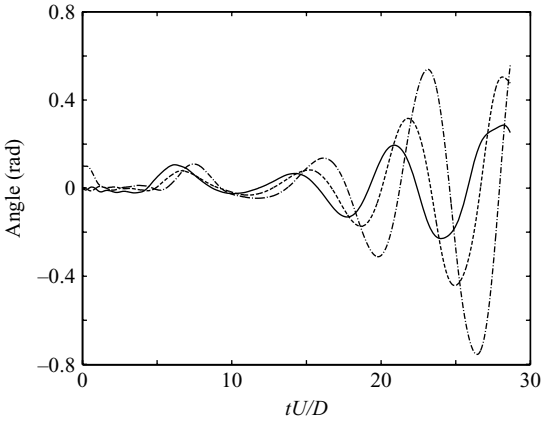

FIGURE 3. Angle with respect to positive X-axis of each constituent body on fish of length $L = 2.275D$. Forebody (—), centrebody (– – –), aftbody (–·–).

The snapshots in figure 2 also depict the instantaneous vectors of the fluid force exerted on each body. These vectors illustrate a general feature of the system that was observed in all cases studied: the wake exerts a force on the forebody with a significant component directed toward the cylinder, while the force on the aftbody is primarily directed downstream.

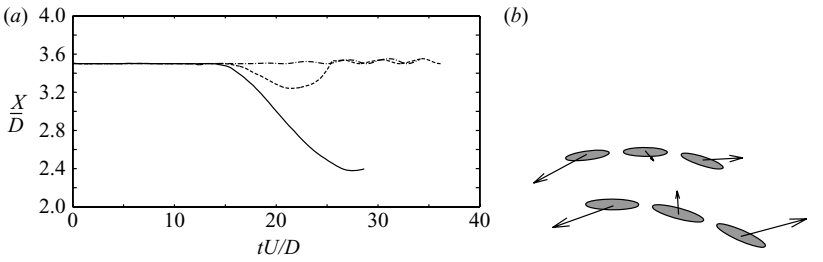

FIGURE 4. (*a*) Horizontal position of 'head' (left-most point) of free-hinge fish of three different lengths. $L = 2.275D$ (—), $L = 2.65D$ (– – –), $L = 3.4D$ (–·–). (*b*) Configurations and instantaneous force vectors on fish of length $L = 2.275D$ (top) and $L = 2.65D$ (bottom) at $tU/D = 20$.

3.1. *Varying body length*

The oppositely directed forces exhibited in figure 2 suggest a 'tug-of-war' whose balance is related to the length of the fish. Indeed, as figure 4(*a*) indicates, as the length of the fish is increased from $L = 2.275D$ to $L = 2.65D$, the fish's upstream displacement is reduced to approximately $0.3D$, and is eventually cancelled. A fish of length $3.4D$ makes no significant motion toward the cylinder. This behaviour can be understood most clearly by examining the snapshots in figure 4(*b*) of fish of length $L = 2.275D$ and $2.65D$, respectively, at the same instant. While the fluid force on the forebody of each fish is similar in magnitude and direction, the force on the aftbody is significantly stronger on the longer fish. As will be discussed below, the force on the aftbody is primarily due to skin friction, which increases with the length of this body, and consequently, with the length of the fish.

It is noted in passing that simulations were also carried out with a single elliptical body with the same dimensions as one of the constituent bodies in the $L = 2.275D$ case, but the results have been omitted for brevity. This body failed to remain stably trapped between the vortices and was instead ejected from the wake. This suggests that there is also a minimum length – probably determined by the size of the passing vortices – for which stable upstream propulsion is possible.

3.2. *Flexible versus rigid structure*

The results of the previous section indicated that the passing vortical flow has a substantial effect on the shape of the free-hinge fish, imparting it with an undulatory motion that is reminiscent of the basic propulsion mode of elongated swimmers (Lighthill 1971; Eldredge 2006). It is natural to enquire whether such shape change is necessary for achieving displacement toward the obstacle. To address this, a fish of length $L = 2.275D$, but with locked hinges, is placed in the flow in the same manner as the previous cases. The trajectories of the centre of mass for both the free- and locked-hinge fish are depicted in figure 5. It is perhaps surprising to find that the trajectories are remarkably similar, and that the locked-hinge fish is actually propelled slightly closer to the cylinder over the same interval. The slight disadvantage of the flexible fish is due to an increased form drag on the aftbody, which becomes more significantly skewed with respect to the flow than in the locked-hinge fish.

While the centres of mass behave similarly, the transverse motion of the fish's head differs significantly between the free- and locked-hinge fish (figure 6). The head of the locked-hinge fish undergoes a larger, and slightly delayed, oscillatory excursion from side to side compared to the free-hinge fish. The flexibility of the latter mitigates the buffeting caused by the passing vortices, whereas the rigid structure of the locked-hinge

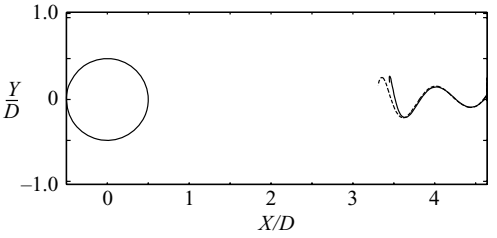

FIGURE 5. Trajectory of centre of mass for fish of length $L = 2.275D$, up to $tU/D = 28.65$. Free hinges (—); locked hinges (– – –).

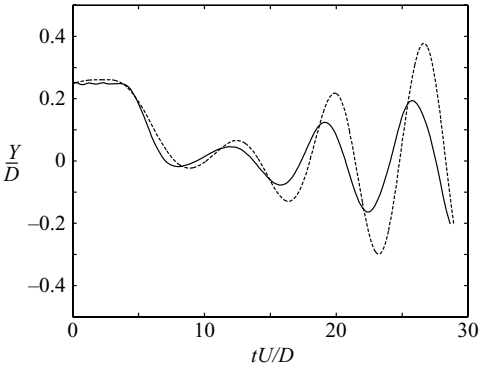

FIGURE 6. Vertical position of head of fish of length $L = 2.275D$. Free hinges (—); locked hinges (– – –).

fish causes it to be rotated more vigorously about its centre of mass. This behaviour of the locked-hinge fish is more apparent in the snapshots and corresponding force vectors shown in figure 7. A particularly strong force is directed toward the centre of a vortex as it passes the fore- and centrebody. This force, after a short delay, pulls the fish's head and then middle portion toward the side on which the vortex has passed. The force on the aftbody, in contrast, is primarily directed along the length of the body.

3.3. *Decomposition of fluid forces*

As discussed previously, the ambient vortical wake exerts competing forces on the fish. To highlight this competition more clearly, the streamwise component of the resultant force on the locked-hinge fish is decomposed into viscous and pressure contributions in figure 8. The locked-hinge fish is considered here for simplicity; the behaviour of forces on the free-hinge fish is similar. Note that only the interval for which the fish moves toward the cylinder is shown. It is apparent from this figure that the pressure contribution is primarily directed upstream (propelling), while the viscous contribution is principally downstream (dragging). Both contributions are falling in magnitude, and at approximately $tU/D = 21.2$, the overall force changes sign from negative to positive, indicating that the fish's forward motion is decelerating.

In figure 9, both the viscous and pressure contributions are decomposed body by body. The most striking feature in the viscous force decomposition in figure 9(a) is that the skin friction on the forebody tends to be directed upstream, and thereby offsets the dominant downstream contributions from the centre and aftbodies. This behaviour is consistent with the fish's intersection with the evolving suction zone, in

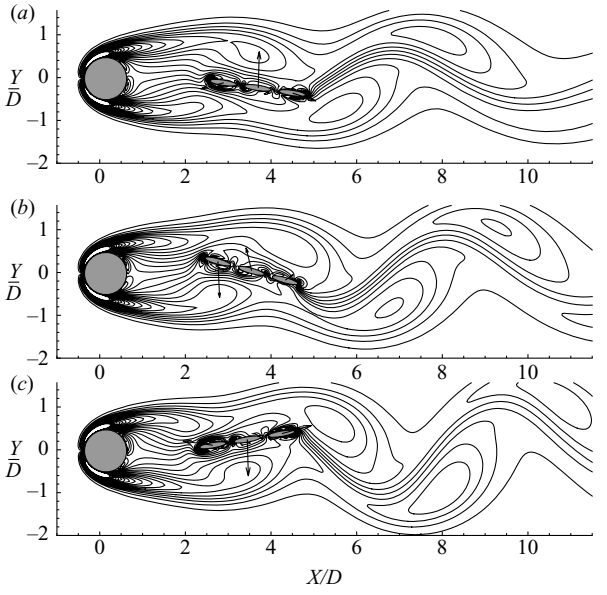

FIGURE 7. Snapshots of the configuration and vorticity field for a locked-hinge fish of length $L = 2.275D$ at three different instants: (*a*) $tU/D = 24.64$, (*b*) 26.40, (*c*) 28.08. Instantaneous force vectors on each constituent body are also shown.

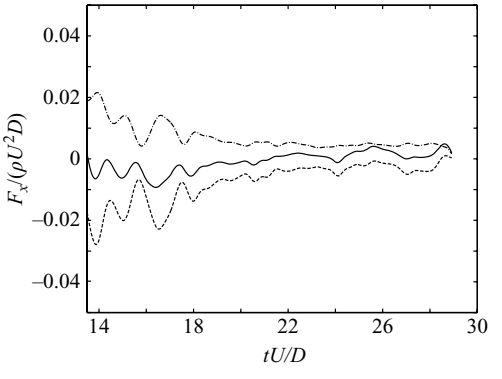

FIGURE 8. Breakdown of X-component of force on locked-hinge fish into viscous (–·–), pressure (– – –), and total (—) contributions.

which the velocity field has an upstream-directed component. This zone is discussed in § 3.4.

The values of both force contributions on the fore- and aftbody tend to oscillate strongly after $tU/D = 20$, when large-scale alternating vortex shedding has begun in earnest. The pressure component in figure 9(*b*) exhibits similar characteristics, though in the early stages, leading-edge suction on the forebody tends to dominate base suction on the aftbody. Once the fish's body is significantly skewed with respect to the flow after $tU/D = 20$, these leading- and trailing-edge contributions are overwhelmed by oscillatory form drag and thrust on all three bodies.

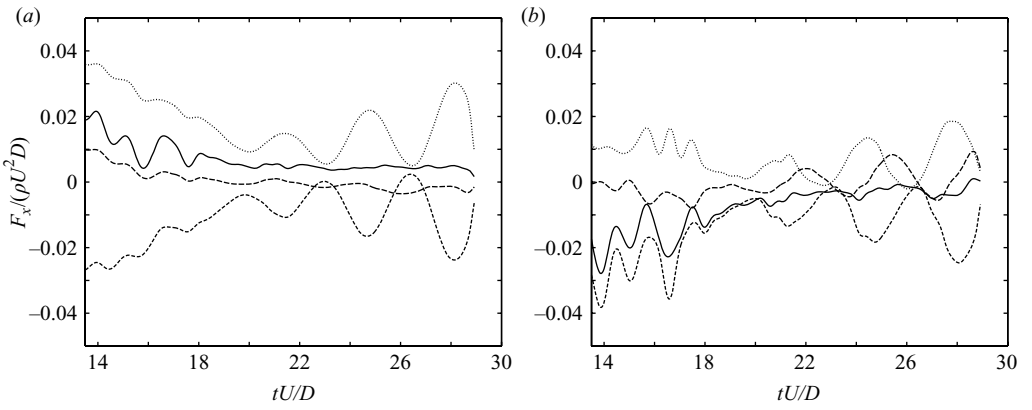

FIGURE 9. (*a*) Viscous and (*b*) pressure contributions to X-component of force on locked-hinge fish, decomposed into individual body's contributions. Forebody (– – –), centrebody (–·–), aftbody (· · ·), total (—).

3.4. *The effect of other parameters*

This paper has focused on the effects of length and flexibility of the fish on its resulting passive propulsion. Studies of these parameters have revealed the influence of leading-edge suction and the passing vortices shed from the obstacle on the forebody, in competition with the skin friction acting on the aft portion of the fish. It is likely that this competition is present in some form in all passive systems in vortical wakes. However, it is important to note that two parameters that have been neglected here, the initial separation ratio d/D and the Reynolds number, will also have important impacts on the behaviour. The range of suitable values of d/D which lead to passive propulsion at this Reynolds number may be partly inferred by observing the instantaneous streamline patterns in figure 10(a, b). The vortices within four diameters of the cylinder significantly deflect the flow, and the zone of reverse flow (the 'suction zone') is demarcated by the indicated level set of zero streamwise velocity.

This suction zone is significantly longer than in the absence of a fish. Figure 10(c) depicts the suction zone and streamline pattern in a fully developed wake behind a cylinder at $Re = 100$ with no fish present. The length of the zone is approximately two diameters, half of its length with a fish present. This behaviour is consistent with previous studies of the effect of wake insertions. The suction zone is substantially the same as the vortex formation region, whose length is defined by the point at which entrained fluid first crosses the midplane of the cylinder (Gerrard 1966). A wide range of experimental data from bluff bodies without wake interference (Unal & Rockwell 1988*a*; Roshko 1993) has shown that the formation length is generally less than two or three diameters. However, the presence of a wake insertion can have a significant effect on the near-wake development. Unal & Rockwell (1988*b*), for example, showed that the vortex formation length actually increases as a rigid splitter plate is brought closer than five diameters. Such a delay in vortex roll-up is apparent in the long shear layers that extend behind the cylinder in figures 2 and 7.

Once roll-up is initiated, the subsequent vortex dynamics are also notably affected by the presence of the fish. In particular, the Strouhal number, fD/U, is markedly lower with a fish present than without. Here, f is defined as the frequency at which vortices pass a given fixed station. Only a few such cycles are observable in the flexible or locked-hinge fish cases; the Strouhal number is approximately 0.142 or

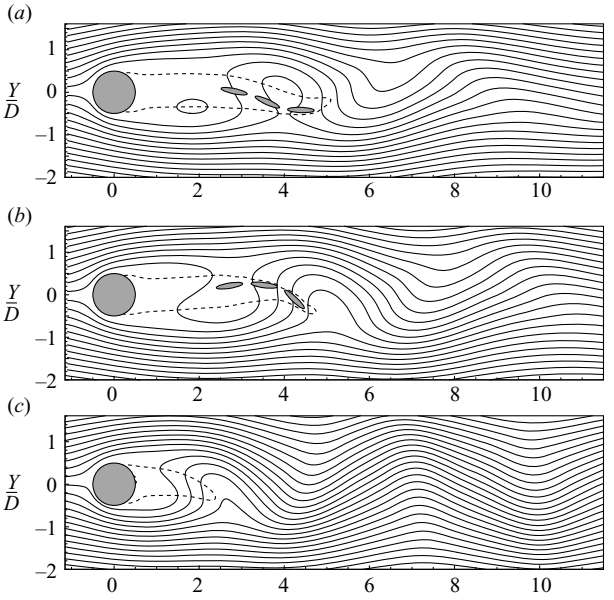

FIGURE 10. Streamline plots and instantaneous free-hinge fish configurations at two instants: (*a*) $tU/D = 24.64$, (*b*) 26.4. Dashed line denotes level set of zero streamwise flow velocity. (*c*) Same flow quantities with no fish present, at $tU/D = 27.3$.

0.136, respectively, compared with 0.164 observed for a cylinder at the same Reynolds number with no wake insertion (both in present simulations and by Williamson 1988).

These observations suggest that the dynamics of the forming wake are coupled with those of the fish, and it may be useful to regard the fish and cylinder as a combined system. This perspective is different from that of Beal *et al.* (2006), who regarded the fish as immersed in a fully developed wake. The wake formation in their higher *Re* experiments was not explored; as mentioned earlier, their measurements of the length of the suction zone were apparently made in the absence of the fish. It is conceivable that the presence of the dead fish at four diameters downstream would extend the length of the suction zone, but it is inappropriate to speculate on this based on the present two-dimensional results at much lower Reynolds number. We postulate that, at Reynolds numbers of order 100, sustained forward displacement or station-keeping are only achievable if the initial position of the fish substantially intersects this formation region. This is the subject of ongoing study.

4. Conclusions

This paper has presented high-fidelity numerical simulations of a simple passive deformable system in the wake of an obstacle. It has been shown that, for certain ratios of body length to cylinder diameter, the fish-like system is passively propelled upstream toward the cylinder. This result is similar to the observations made by Beal *et al.* (2006) in their experiments with a dead fish, though in this earlier investigation the additional thrust was attributed to the body flapping induced by the wake. In the present study, the additional thrust arises from a combination of mechanics at the head of the fish, namely, leading-edge suction and upstream-oriented skin friction, which overcome the streamwise skin friction on the aft portion. The region behind

the cylinder in which this suction is available is greatly extended by the presence of the fish. As demonstrated in this paper, these mechanics work equally well when the fish is rigid.

There are several aspects of this problem that are beyond the scope of this paper but warrant further study. The initial placement of the fish – longitudinal and lateral – has not been systematically explored, and it would be interesting to determine whether there exists an equilibrium position at which the fish can hold station indefinitely. Secondly, the passive body may have a significant influence on the drag of the upstream cylinder, but this has not been investigated here. Finally, the degree of coupling in the dynamics of the wake–fish system must be explored further. In light of the transverse oscillations exhibited by the inserted body, it would be interesting to classify the present system in the taxonomy of vortex-induced vibrations, and bring to bear some of the tools applied to such problems (Williamson & Govardhan 2004).

Support for this work by the National Science Foundation, under award CBET-0645228, is gratefully acknowledged.

REFERENCES

Allen, J. J. & Smits, A. J. 2001 Energy harvesting eel. *J. Fluids Struct.* **15**, 629–640.

Beal, D. N., Hover, F. S., Triantafyllou, M. S., Liao, J. C. & Lauder, G. V. 2006 Passive propulsion in vortex wakes. *J. Fluid Mech.* **549**, 385–402.

Eldredge, J. D. 2006 Numerical simulations of undulatory swimming at moderate Reynolds number. *Bioinspir. Biomim.* **1**, S19–S24.

Eldredge, J. D. 2008 Dynamically coupled fluid–body interactions in vorticity-based numerical simulations. *J. Comput. Phys.* doi: 10.1016/j.jcp.2008.03.033.

Fausch, K. D. 1993 Experimental analysis of microhabitat selection by juvenile steel head (*Oncorhynchus mykiss*) and coho salmon (*O. kisutch*) in a British Columbia stream. *Can. J. Fish. Aquat. Sci.* **50**, 1198–1207.

Fausch, K. D. & White, R. J. 1981 Competition between brook trout (*Salvelinus fontinalis*) and brown trout (*Salmo trutta*) for positions in a Michigan stream. *Can. J. Fish. Aquat. Sci.* **38**, 1220–1227.

Gerrard, J. H. 1966 The mechanics of the formation region of vortices behind bluff bodies. *J. Fluid Mech.* **25**, 401–413.

Liao, J. C., Beal, D. N., Lauder, G. V. & Triantafyllou, M. S. 2003 The Kármán gait: novel body kinematics of rainbow trout swimming in a vortex street. *J. Exp. Biol.* **206**, 1059–1073.

Lighthill, M. J. 1971 Large-amplitude elongated-body theory of fish locomotion. *Proc. R. Soc.* B **179**, 125–138.

Roshko, A. 1993 Perspectives on bluff body aerodynamics. *J. Wind Engng Indust. Aerodyn.* **49**, 79–100.

Unal, M. F. & Rockwell, D. 1988*a* On vortex formation from a cylinder. Part 1. The initial instability. *J. Fluid Mech.* **190**, 491–512.

Unal, M. F. & Rockwell, D. 1988*b* On vortex formation from a cylinder. Part 2. Control by splitter-plate interference. *J. Fluid Mech.* **190**, 513–529.

Webb, P. W. 1998 Entrainment by river chub *Nocomis micropogon* and smallmouth bass *Micropterus dolomieu* on cylinders. *J. Exp. Biol.* **201**, 2403–2412.

Weihs, D. 1973 Hydromechanics of fish schooling. *Nature* **241**, 290–291.

Williamson, C. H. K. 1988 Defining a universal and continuous Strouhal–Reynolds number relationship for the laminar vortex shedding of a circular cylinder. *Phys. Fluids* **31**, 2742–2744.

Williamson, C. H. K. & Govardhan, R. 2004 Vortex-induced vibrations. *Annu. Rev. Fluid Mech.* **36**, 413–455.